CTU Journal of Innovation and Sustainable Development
ISSN 2588-1418 | e-ISSN 2815-6412

DOI:10.22144/ctujoisd.2025.025

Synthesis of cellulose nanofiber from *Nypa fruticans* shell collected from Can Tho City, Viet Nam

Thieu Quang Quoc Viet[1,2], Luong Huynh Vu Thanh[2], Le Thi Cam Tuyen[2], Nguyen Tuan Loi[3,4], Tran Thi Hoang Thy[1], Nguyen Tuyet Ngan[1], and Duong Ho Thai Bao[1]

[1]*Composite Materials Lab, College of Engineering, Can Tho University, Viet Nam*

[2]*Faculty of Chemical Engineering, College of Engineering, Can Tho University, Viet Nam*

[3]*Institute of Fundamental and Applied Sciences, Duy Tan University, Viet Nam*

[4]*Faculty of Environmental and Chemical Engineering, Duy Tan University, Viet Nam*

**Corresponding author (tqqviet@ctu.edu.vn)*

Article info.

Received 26 Jun 2024
Revised 17 Jul 2024
Accepted 20 Dec 2024

Keywords

Cellulose nanofiber, Hydrothermal method, Nypa fruticans, Oxalic acid, Peroxyformic acid

ABSTRACT

In this study, cellulose nanofiber (CNF) was synthesized from Nypa fruticans shells as raw material in Can Tho City. CNF was successfully produced via several steps. Firstly, raw material was treated with a mixture of Peroxyformic acid solution, then with an alkaline solution and bleached. Finally, it was hydrolyzed with 5% oxalic acid combined with hydrothermal and used ultrasonic waves with a high number of 40 kHz. The obtained materials after each step were surveyed and evaluated through advanced analysis methods, such as Fourier transform infrared spectroscopy, X-ray diffraction, thermogravimetric analysis, and scanning electron microscopy. The results indicate that the CNF material had high purity, high crystallinity, and an average size of about 15.74 nm. The results of this study demonstrate the potential of Nypa fruticans shells as a low-cost and environmentally friendly raw material for CNF synthesis.

1. INTRODUCTION

Nypa fruticans, also known as leaf *Nypa fruticans* or mangrove palm, is the only palm species that can live in swamps. It originates from the coasts of the Indian and Pacific Ocean, widely distributed in mangrove forests in South Asia, Southeast Asia, and other regions with saltwater or brackish water environments (Lawrence & Dennis, 1988; Kenvin & Siti, 2000; United States Department of Agriculture, 2024). Parts of the nipa palm tree are used in various ways, such as for food, firewood, and nipa fronds, which are used as composites for medium-density fiberboards (Kruse & Frühwald, 2001). *Nypa fruticans* is a plant commonly grown in Viet Nam. Despite its economic benefits, many *Nypa fruticans* shells are not fully utilized; most are used as a fuel source or discharged directly into the environment, causing pollution. The main components of the *Nypa fruticans* shell are cellulose, hemicellulose, and lignin (Pramila & Shiro, 2011; Wijana et al., 2023). This makes Nypa fruticans shells an abundant carbon source suitable for applications in Lithium-ion batteries.

Cellulose is one of the most common natural polymers in the world and is the main component of plants and algal fibers. Cellulose can be decomposed into a nanometre-sized structure called nano cellulose, which helps improve mechanical properties and adsorption capacity, and increases the number of active -OH functional groups on the surface (An et al., 2021). Nanocellulose from *Nypa fruticans* shells was synthesized through

pretreatment, isolation, bleaching, and hydrolysis. Because the structure of lignocellulose ~~is~~ consists of fiber bundles made up of cellulose bundles surrounded by hemicellulose and lignin, it must undergo steps such as pretreatment, isolation, and bleaching to remove lignin and hemicellulose to create nanocellulose. Finally, only cellulose ~~is~~ was hydrolyzed to produce nanocellulose. Various techniques were used to determine the structure of nanocellulose such as scanning electron microscopy (SEM), X-ray diffraction (XRD), Fourier transform infrared spectroscopy (FTIR), and thermogravimetric analysis (TGA) (An et al., 2020; Fahma et al., 2021).

Cellulose nanofiber (CNF) obtained from *Nypa fruticans* shells exhibits significant potential as a sustainable and biodegradable material, finding applications in various fields such as packaging, textiles, biomedicine, energy storage (Fahma et al., 2021; Sandeep et al., 2021; Khalil et al., 2016). With many excellent physical and chemical properties, CNF is widely used in daily life, including energy storage. Its large surface area and high electrical conductivity make CNF suitable material for supercapacitors (and) batteries.

2. MATERIALS AND METHODS

2.1. Materials

Nypa frutican shells as raw material were collected from Can Tho City, Viet Nam. The chemicals used included oxalic acid dihydrate ($C_2H_2O_4.2H_2O$, ≥ 99.5%), formic acid (HCOOH, ≥ 88.0%), hydrogen peroxide (H_2O_2, ≥ 30%), sodium hydroxide (NaOH, ≥ 96%). All chemicals were purchased from Xilong Scientific Co., Ltd., China, and used without any purification process.

2.2. Methods

2.2.1. Fourier transform infrared spectroscopy

The FTIR spectrum was measured using a Bruker Vertex 70 FTIR spectrometer. The analysis was performed on powder samples in the wave number range from 4000 – 400 cm^{-1}, with a resolution of 4 cm^{-1}.

2.2.2. X-ray diffraction

XRD patterns were measured using an ADVANCE D8 – Bruker device. Samples were measured under operating condition of 40 kV, 40 mA (1,600 W) with a step size of 0.01°, and a step time of 250 seconds, covering the range 20 – 80°.

2.2.3. Thermogravimetric analysis

TGA is an analytical method used to determine the thermal stability and decomposition temperature of nanocellulose. The analysis was conducted using a TAQ500 thermal analysis system. Samples were scanned from 30℃ to 800℃ in a nitrogen atmosphere.

2.2.4. Scanning electron microscope

The method was performed using Hitachi S-4800 equipment. This method is used to analyze the morphology of fiber structure and solid morphology, and it is widely employed in determining the characteristics of materials after processing steps.

2.2.5. Pretreatment of Nypa frutican shells

The pretreatment process is illustrated in Figure 1. In this process, *Nypa fruticans* shells are sorted and washed. Then, the heads of *Nypa fruticans* shells are cut into pieces about 1 cm thick and removed. They are dried at 80℃ for 24 h. After drying, the materials are coarsely ground using an AH-260 chopper and finely ground with an MF 10BS0A0 mill, operating at 230 V, 1000 W, and 50 Hz frequency. After grinding, the resulting material has a diameter of less than 250 micrometers (referred to as raw material).

Figure 1. Diagram of the pretreatment process of *Nypa fruticans* shells

2.2.6. Peroxyformic acid (PFA) treatment

After grinding, the raw material was pretreated with distilled water at a 1/20 (wt/vl) ratio, continuously stirred for 2 h at 90°C and 400 rpm to thoroughly remove dust, dirt, and tannins from the *Nypa fruticans* shells. It was then evenly mixed in the PFA mixture (90% HCOOH + 5% H_2O_2 + 5% H_2O) at a ratio of 1/40 (wt/vl) and stirred continuously at 90°C for 4 h. After stirring, it was filtered and washed

with distilled water several times until reaching a neutral pH.

2.2.7. Bleaching

Samples after PFA treatment were subsequently treated with an alkaline solution using 0.5 M NaOH. This process was conducted at 70°C with stirring for 4 h and adjusted to pH ≈ 12. After alkaline treatment, multiple filtrations were performed, followed by bleaching with 30% H_2O_2 at a ratio of 4/1 (wt/wt) at 80℃ for 1 h. The objective of this process was to remove lignin and hemicellulose completely. The samples were washed with hot water and filtered using a vacuum filtration system after each treatment. Following these treatments, the resulting sample consisted of pure cellulose.

2.2.8. Hydrothermal treatment

The bleached mixture was treated using an autoclave as a hydrothermal treatment technique combined using hydrolysis with 5% oxalic acid dihydrate (HOOC-COOH) at a ratio of 1/10 (wt/vl) at 160℃ for 4 h. Subsequently, the sample was sonicated using an Ultrasonic Cleaner (TUC-20) with a power of 60 W and a frequency of 40 kHz for 30 min at 50°C. After this process, the sample was filtered and centrifuged at 4500 rpm three to four times until it reached a neutral pH. The sample was then freeze-dried by freezing it at −80°C for 3 h and drying it for 24 h at 30°C. The product obtained after drying is CNF.

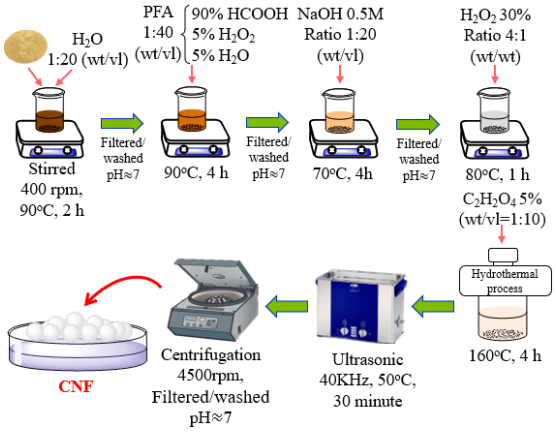

Figure 2. Schematic illustration for the synthesis of CNF from *Nypa fruticans* shells

3. RESULTS AND DISCUSSION

3.1. Fourier transform infrared spectroscopy

FTIR analysis provides information about the chemical structure by determining the vibrations of chemical functional groups present in the sample. Figure 3 shows the FTIR spectrum of the samples at each stage, revealing two main absorption regions: one at low wavenumbers ranging from 1800 to 700 cm^{-1} and another at higher wavenumbers around 3500-2700 cm^{-1}, related to the vibrations of the OH group. Particularly, the OH group spectrum peak exhibits a bulb shape, a wide spectral base, and high transmittance, indicating the presence of hydroxyl groups on the surface and intermolecular hydrogen bonds between chains (Prado & Spinacé, 2019; Hai et al., 2020; Ma et al., 2023). Additionally, absorption is observed around 2900 - 2800 cm^{-1} and approximately 1500 - 1250 cm^{-1}, representing the C-H bonds present in cellulose, hemicellulose, and lignin compositions. (Prado & Spinacé, 2019). Specifically, lignin shows a characteristic absorption peak in the of 1600 - 1500 cm^{-1} range of the C=O group, corresponding to the vibrations of the acetyl groups in lignin and hemicellulose (Prado & Spinacé, 2019; Ma et al., 2023). Peaks in the wave number range of 1161 - 1030 cm^{-1} correspond to the stretching vibration of the C-O bond and the deformation vibration of the C-H bond in the pyranose ring of cellulose (Trilokesh & Uppuluri, 2019; Ma et al., 2023).

Through the processing from the original raw sample to the bleached sample, the characteristic spectral peaks of the functional groups in the lignin and hemicellulose components gradually disappeared, indicating that all the impurities were removed after the bleaching process. Only the amorphous part remained, consisting of pure cellulose. Upon comparing the FTIR spectra of the bleached sample and CNF, it becomes evident that the spectral peaks characteristic of the cellulose bonds, such as O–H bond, the bond in the pyranose ring, and the β-glucoside bond, exhibited reduced intensity (Zhao et al., 2019; An et al., 2020).

Based on the above results, it is concluded that no lignin or hemicellulose was present in the CNF sample. This is evident specifically in the absence of absorption peaks associated with these components. Furthermore, acid hydrolysis, combined with the hydrothermal method, effectively removed impurities, leaving behind concentrated cellulose. The absorption peaks observed in the range of 900 - 620 cm^{-1} indicate the presence of C-OH bonds, C-O-C and C-C interactions within the crystal structure resulting in relatively weak absorption peaks (An et al., 2020; An et al., 2021). FTIR analysis reveals fluctuations in functional groups of the material after processing stages, similar to those

in the raw sample. However, the vibration at 1060 cm^{-1} characterizes the C-O functional groups in the cellulose structure with higher intensity compared to the raw sample. This suggests that processing removes components like lignin, hemicellulose, or other impurities, resulting in cellulose with increased purity.

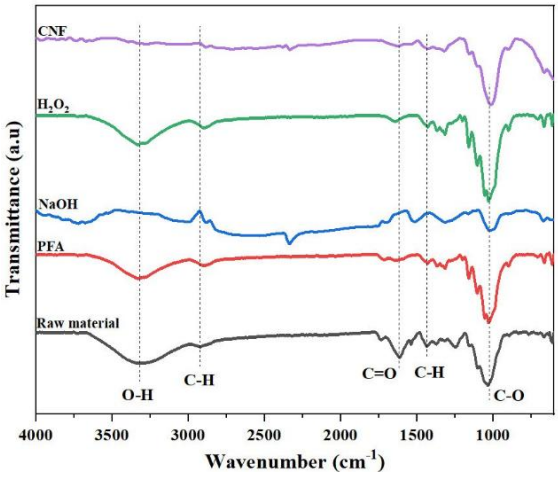

Figure 3. FTIR spectra of raw material, material after treatment with PFA, NaOH, H_2O_2, and CNF material

3.2. X-ray diffraction

Figure 4 shows the XRD diagram of raw material, samples after treatment with PFA, NaOH, H_2O_2, and CNF material. According to theory, the XRD pattern of pure cellulose is characterized by three diffraction peaks at angles 2θ with values of 15.4°, 22.5° and 34.6° respectively (Liu et al., 2010; Park et al., 2019; Yadav et al., 2021; Ma et al., 2023). From the raw material to the bleached material, the intensity of the diffraction peak gradually increases, with a prominent shift observed in the peak at 2θ of approximately 22.5°. The CNF sample demonstrated significantly higher crystallinity compared to the other samples, as evidenced by the pronounced peak at approximately 22.5°. This demonstrates that impurities and amorphous fractions, including hemicellulose and lignin, were completely removed through the processing stages. Therefore, the XRD results obtained are consistent with the FTIR results analyzed earlier.

Comparing the XRD patterns of the bleached material and CNF material reveals a sharp decrease in the intensity of the diffraction peak around 2θ approximately 22.5°. This observation indicates that the crystallinity of CNF decreased after undergoing acid hydrolysis combined with the hydrothermal method. Cellulose, being a semi-crystalline polymer, with alternating crystalline and amorphous regions, undergoes selective attack by H^+ ions during acid hydrolysis. These ions primarily target and break the β-1,4-O-glucoside bonds in the amorphous region, thereby reducing the CNF chain length and fiber size (Rhim et al., 2015; Wang et al., 2019). XRD analysis revealed no peaks associated with impurities in the treated material. This finding suggests that the chemical treatments effectively removed impurities present in the original material.

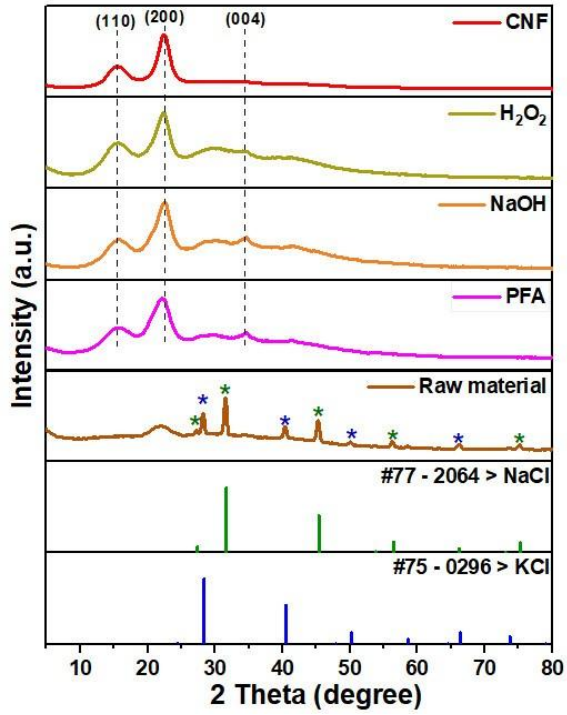

Figure 4. XRD patterns of raw material, material after treatment with PFA, NaOH, H_2O_2 and CNF material

3.3. Thermogravimetric analysis

The TGA results of the raw material are presented in Figure 5, indicating an initial mass decrease of approximately 5.64% in the temperature range from 60 to 150°C, attributed to the evaporation of water molecules and impurities present in the raw sample. Subsequently, there is a sharp mass decrease between 200 and 400°C, resulting in a loss of about 40.93% (Kim et al., 2019). This significant mass loss during this phase is due to the decomposition of lignin and hemicellulose, which initiates around 323°C (An et al., 2020). The decomposition process generates a char layer that envelops the cellulose structure, acting as a fire-retardant agent that slows

the contact between cellulose fibers and heat sources, thereby prolonging the cellulose decomposition process. At approximately 460°C, an additional 12.48% mass loss occurs due to the decomposition of the char layer, followed by a further decrease of 17.03% in mass around 485°C, indicating the onset of cellulose decomposition (An et al., 2020).

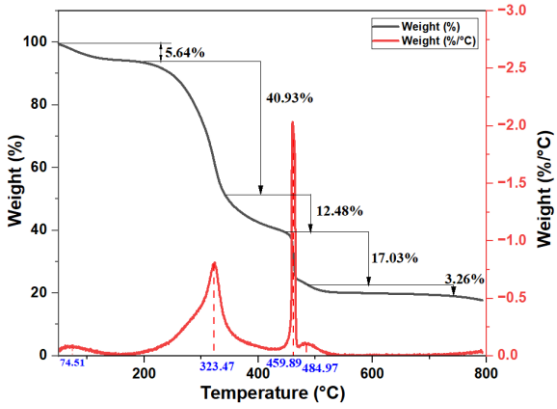

Figure 5. TGA diagram of raw material

The TGA analysis of the CNF material is shown in Figure 6. The results indicate that the mass of CNF begins to decrease in the range of 80 to 200°C due to evaporation of water molecules present in the CNF (An et al., 2020). Subsequently, nanocellulose rapidly decomposes in the temperature range of 250 to 450°C, reaching peak decomposition at 380°C, with a mass loss of approximately 70.99% (An et al., 2020). The removal of the amorphous region, including lignin and hemicellulose, during the processing stages results in a nanocellulose material that exhibits lower thermal stability compared to the original raw material sample (An et al., 2020). Between 450 and 600°C, there is a further mass loss of about 24.47% due to the decomposition of impurities and residual cellulose, ultimately leading to complete decomposition of the CNF (An et al., 2020). TGA analysis of the CNF compared to the raw material indicated high purity of the obtained product, with negligible amounts of impurities detected.

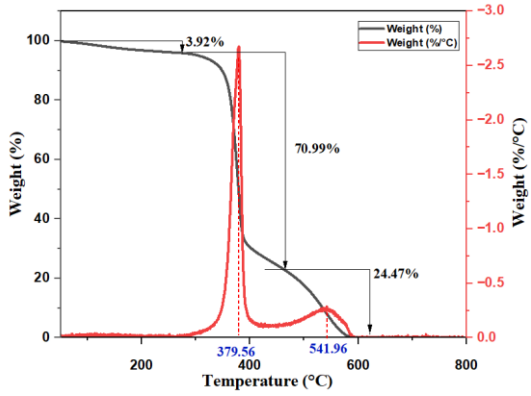

Figure 6. TGA diagram of CNF sample

3.4. Scanning electron microscope

The results of morphological analysis using the SEM method are shown in Figure 7. The SEM image analysis in Figure 7(a) of the raw material reveals that the fiber surface has a textured shape due to the tightly interconnected outer layers, which include lignin, hemicellulose, pectin, wax, and oil. In Figure 7(b), the bleached cellulose fiber produced from the raw material shows that the fiber bundles have been separated into extremely small-sized fibers, confirming that hemicellulose and lignin present in the raw material have been successfully removed. These results are consistent with the findings from XRD and FTIR analyses (Xing et al., 2022; Zhang et al., 2020).

The SEM image of the CNF material (Figure 7(c)) demonstrates that the CNF material has achieved the desired nanostructure size. Figure 7(d) reveals that CNF is in the form of long fibers with an average diameter of 15.74 nm, produced through a hydrothermal process combined with acid hydrolysis. Through the processing stages, the amorphous regions in the structure have been eliminated. Additionally, under the effect of hydrothermal treatment and ultrasonic treatment, the CNFs are broken, and their size is reduced due to the impact of temperature, high pressure, and ultrasonic waves. The CNFs are distributed in an interwoven network, forming CNF sheets. Combined analysis by FTIR, XRD, and TGA strongly suggests a high degree of purity in the obtained CNF.

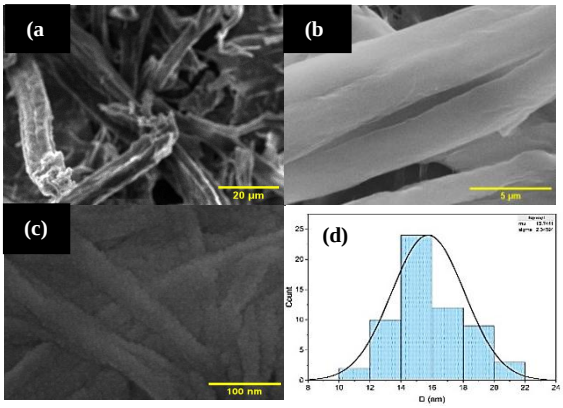

Figure 7. SEM images of samples (a) Raw material, (b) Cellulose, (c) CNF (d) Diameter distribution

4. CONCLUSION

In this study, CNF was successfully synthesized from *Nypa fruticans* shells using a combination of chemical treatments with hydrothermal methods. The chemical treatment process effectively removed hemicellulose, lignin and other impurities in *Nypa fruticans* shells, yielding pure cellulose. Subsequent hydrothermal processing facilitated the conversion of cellulose into CNF under controlled pressure, temperature, and acidic conditions. The study provides a comprehensive analysis of the synthesized materials properties, including crystallinity, functional groups, and thermal stability. The obtained CNF possesses high crystallinity, with diameters ranging from 1 to 100 nm, and an average size of approximately 15.74 nm. These characteristics suggest that CNF derived from *Nypa fruticans* shells holds significant potential for applications in supercapacitors and batteries. Furthermore, this research highlights the environmental benefits of recycling agricultural by-products, specifically *Nypa fruticans* shells, into valuable nanomaterials, thereby contributing to sustainable resource utilization and waste reduction.

ACKNOWLEDGMENT

This research is funded by the Ministry of Education and Training of Viet Nam under grant number B2023-TCT-04.

REFERENCES

An, V. N., Nhan T. H. C., Tap D. T., Van T. T. T., Viet P. V., & Hieu L. V. (2020). Extraction of high crystalline nanocellulose from renewable sources of Vietnamese agricultural wastes. *Journal of Polymers and the Environment*, *28*(6), 1465-1474. https://link.springer.com/article/10.1007/s10924-020-01695-x

Fahma, F., Febiyanti, I., Lisdayana, N., Arnata, I. W., & Sartika, D. (2021). Nanocellulose as a new sustainable material for various applications: A review. *Archives of Materials Science and Engineering*, *109*(2), 49-64. http://dx.doi.org/10.5604/01.3001.0015.2624

Hai, L. V., Zhai, L., Kim, H. C., Panicker, P. S., Pham, D. H., & Kim, J. (2020). Chitosan Nanofiber and Cellulose Nanofiber Blended Composite Applicable for Active Food Packaging. *Nanomaterials (Basel, Switzerland)*, *10*(9), 1752. http://dx.doi.org/10.3390/nano10091752

Kenvin, H. D., & Siti, A. A. (2000). Biodiversity and distribution of fungi associated with decomposing Nypa fruticans. *Biodiversity & Conservation*, *9*, 393-402. http://dx.doi.org/10.1515/9783110264067.273

Khalil, H. A., Davoudpour, Y., Saurabh, K. S., Hossain, M. S., Adnan, A. S., Dungani, R., Paridah, M., Sarker, M. Z. I., Fazita, M. R. N., Syakir, M. I., & Haafiz, M. K. M. (2016). A review on nano cellulosic fibers as new material for sustainable packaging: Process and applications. *Renewable and Sustainable Energy Reviews*, *64*, 823-836. http://dx.doi.org/10.1016/j.rser.2016.06.072

Kim, H. G., Lee, U. S., Kwac, L. K., Lee, S. O., Kim, Y. S., & Shin, H. K. (2019). Electron beam irradiation isolates cellulose nanofiber from Korea "Tall Goldenrod" invasive alien plant. *Nanomaterials (Basel, Switzerland)*, *9*(10), 1358. https://doi.org/10.3390/nano9101358

Kruse, K.M., & Frühwald, A. (2001). *Properties of Nipa-and Coconut fibers and production and properties of particle-and MDF-boards made from nipa and coconut. Johann Heinrich von Thünen-Institut (vTI), Bundesforschungsinstitut für Ländliche Räume, Wald und Fischerei*.

Lawrence, H. S., & Dennis, M. H. (1988). Use and management of Nipa palm (Nypa fruticans, Arecaceae): A review. *Economic Botany*, *42*, 206-213. https://doi.org/10.1007/bf02858921

Liu, D., Zhong, T., Chang, P. R., Li, K., & Wu, Q. (2010). Starch composites reinforced by bamboo cellulosic crystals. *Bioresource Technology*, *101*(7), 2529-2536. http://dx.doi.org/10.1016/j.biortech.2009.11.058

Ma, Y., Chai, X., Bao, H., Huang, Y., & Dong, W. (2023). Study on nanocellulose isolated from waste

chili stems processing as dietary fiber in biscuits. *Plos one*, *18*(1). http://dx.doi.org/10.1371/journal.pone.0281142

Park, NM., Choi, S., Oh, J. E., & Hwang, D. Y. (2019). Facile extraction of cellulose nanocrystals. *Carbohydrate Polymers*, *223*, 114115. http://dx.doi.org/10.1039/C5GC02576A

Prado, K. S., & Spinacé, M. A. S. (2019). Isolation and characterization of cellulose nanocrystals from pineapple crown waste and their potential uses. *International journal of biological macromolecules*, *122*, 410-416. http://dx.doi.org/10.1016/j.ijbiomac.2018.10.187

Pramila, T., & Shiro, S. (2011). Chemical characterization of various parts of nipa palm (*Nypa fruticans*). *Industrial Crops and Products*, *34*(3), 1423-1428. http://dx.doi.org/10.1016/j.indcrop.2011.04.020

Rhim, JW., Reddy, J. P., & Luo, X. (2015). Isolation of cellulose nanocrystals from onion skin and their utilization for the preparation of agar-based bio-nanocomposites films. *Cellulose*, *22*(1), 407-420. http://dx.doi.org/10.1007/s10570-014-0517-7

Sandeep, A. S., Aditya, S. R., Swarnim, B. S., & Alain, D. (2021). Nanocellulose in food packaging: A review. *Carbohydrate Polymers*, *255*, 1-17. http://dx.doi.org/10.1016/j.carbpol.2020.117479

Trilokesh, C., & Uppuluri, K. B. (2019). Isolation and characterization of cellulose nanocrystals from jackfruit peel. *Sci Rep*, *9*. https://www.nature.com/articles/s41598-019-53412-x

United States Department of Agriculture. (2024). Nypa fruticans Wurmb. https://npgsweb.ars-grin.gov/gringlobal/taxon/taxonomydetail?id=25449

Wang, Z., Yao, Z., Zhou, J., He, M., Jiang, Q., Li, S., Ma, Y., Liu, M., & Luo, S. (2019). Isolation and characterization of cellulose nanocrystals from pueraria root residue. *International journal of biological macromolecules*, *129*, 1081–1089. http://dx.doi.org/10.1080/15440478.2020.1821292

Wijana, S., Setyawan, H. Y., Wan, Z., Zhu, M., Pranowo, D., Dewi, I. A., & Nareswari, M. P. (2023). The potential of Nypa Frutican as an energy source in Indonesia: A Review. *Advances in Food Science, Sustainable Agriculture and Agroindustrial Engineering (AFSSAAE)*, *6*(1), 88-96. http://dx.doi.org/10.21776/ub.afssaae.2023.006.01.8

Xing, H., Fei, Y., Cheng, J., Wang, C., Zhang, J., Niu, C., Fu, Q., Cheng, J., & Lu, L. (2022). Green Preparation of Durian Rind-Based Cellulose Nanofiber and Its Application in Aerogel. *Molecules (Basel, Switzerland)*, *27*(19), 6507. http://dx.doi.org/10.3390/molecules27196507

Yadav, H. M., Park, J. D., Kang, H. C., Kim, J., & Lee, J. J. (2021). Cellulose Nanofiber Composite with Bimetallic Zeolite Imidazole Framework for Electrochemical Supercapacitors. *Nanomaterials (Basel, Switzerland)*, *11*(2), 395. http://dx.doi.org/10.3390/nano11020395

Zhang, C., Jiang, Q., Liu, A., Wu, K., Yang, Y., Lu, J., Cheng, Y., & Wang, H. (2020). The bead-like $Li_3V_2(PO_4)_3$/NC nanofibers based on the nanocellulose from waste reed for long-life Li-ion batteries. *Carbohydrate Polymers*, *237*(3-4), 116-134. http://dx.doi.org/10.1016/j.carbpol.2020.116134

Zhao, G., Du, J., Chen, W., Pan, M., & Chen, D. (2019). Preparation and thermostability of cellulose nanocrystals and nanofibrils from two sources of biomass: rice straw and poplar wood. *Cellulose*, *26*, 8625-8643. https://link.springer.com/article/10.1007/s10570-019-02683-8